energies

MDPI

Article

Numerical Simulations of DDT Limits in Hydrogen-Air Mixtures in Obstacle Laden Channel

Wojciech Rudy * and Andrzej Teodorczyk

Institute of Heat Engineering, Faculty of Power and Aeronautical Engineering, Warsaw University of Technology, Nowowiejska 21/25, 00-665 Warsaw, Poland; andrzej.teodorczyk@pw.edu.pl
* Correspondence: wojciech.rudy@pw.edu.pl

Abstract: The main aim of this study was to perform numerical simulations of deflagration to detonation transition process (DDT) in hydrogen–air mixtures and assess the capabilities of freeware open-source ddtFoam code to simulate and capture DDT limits. The numerical geometry was based on the real 0.08 × 0.11 × 4 m (H × W × L), rectangular cross-section detonation channel previously used to experimentally investigate DDT limits in obstacle-filled channel. The constant blockage ratio (BR) equal to 0.5 was kept for three obstacle spacing configurations: S = H, 2H, 3H. The results showed that hydrogen concentration limits for successful DDT from simulations are close to the experimental values, however, the simulated DDT limits range is wider than the experimental one and depends on the obstacles spacing. The numerical results were analyzed by means of propagation velocities, overpressures, and run-up distances. The best match between numerical and experimental DDT limits was observed for obstacles spacing L = 3H and the lowest match for spacing L = H. The comparison between experimental and numerical results points at the possible application of ddtFoam in geometry with a relatively low level of congestion. This work results proved that simulations in such geometry provide numerical flame acceleration velocity profiles, run-up distance, and recorded overpressures very close to experimentally measured.

Keywords: DDT; hydrogen-air; ddtFoam; DDT limits; obstacle laden tube

Citation: Rudy, W.; Teodorczyk, A. Numerical Simulations of DDT Limits in Hydrogen-Air Mixtures in Obstacle Laden Channel. *Energies* **2021**, *14*, 24. https://dx.doi.org/10.3390/en14010024

Received: 23 November 2020
Accepted: 21 December 2020
Published: 23 December 2020

1. Introduction

Hydrogen as a carbonless and environmentally friendly fuel is considered as the future energy carrier. Its properties such as wide flammability limits, high laminar burning velocity (in air ~2.5 m/s), low ignition energy (in air ~0.02 mJ), and high lower heating value (~120 MJ/kg) point at a variety of possible hydrogen applications. However, the listed advantages of hydrogen properties might be also considered as disadvantages from the safety point of view. In the case of unintended leakage, hydrogen is easier to ignite under wider concentration conditions, and after ignition, flame will propagate faster. Additionally, the hydrogen–air flame is inherently unstable and if the conditions are favorable the hydrogen flame might go through the deflagration to detonation transition (DDT) process. As the DDT process depends on a variety of parameters (fuel concentration, congestion presence, and its geometrical configuration), it is crucial to investigate these parameters' influence to prevent DDT in common use. As the experimental investigation is expensive in terms of time and cost, Computational Fluid Dynamics (CFD) codes have been developed to solve complex numerical problems. Nowadays, CFD analysis is applied in many branches of industry such as aerospace, automotive, power generation, manufacturing, petrochemical, process safety, turbomachinery, etc. The main advantage of using CFD simulations is to reduce the time of the designing process and, simultaneously, detailed numerical models might be used to get a better insight into the process that is difficult to investigate experimentally. DDT is one of such processes as it combines a wide range of flame propagation velocities (0–2000 m/s). Therefore, depending on the flame velocity,

the interactions among chemical kinetics, flame, unburned mixture, turbulence, and shock waves are at a different level of complexity.

DDT process in hydrogen–air mixtures has been extensively investigated experimentally [1–13] and numerically [14–21] over the course of 30 years. The essential condition for the planar detonation front to propagate stably is the presence of developed cellular structure, so it is possible to correlate the characteristic cell size width λ with the characteristic dimension of the channel which might be defined in various ways. For example, based on the extensive research, Dorofeev et al. [1] provided the critical correlation of $L/\lambda \approx 7$, where L is the characteristic dimension of the experimental setup that might be interpreted as the minimum distance for detonation formation. Dimension L is, therefore, correlated with blockage ratio and obstacle spacing value. The methodology for calculation of the L value depending on the channel geometry is described in Reference [1]. The criterion was further confirmed by studying the blockage ratio influence on the DDT in a CH_4–air mixture [10]. It has been also proven that DDT limits are experimental stand scale-dependent as the lower concentration limit for successful DDT was decreasing with the increase of the scale of the setup. Sample measurements of lower limits in a 30.5 cm [11], 43 cm [22] diameter tubes, and 2.3 m high channel [23] gave values of 15%, 13.6%, and 12.5% of hydrogen in air, respectively. As the cost of experiments increases significantly with the scale of the experimental setup, the numerical simulations have become attractive, low-cost tools to investigate flame acceleration and transition to detonation.

One of the recent numerical codes designed and tested in a variety of scales and hydrogen–air mixtures composition is ddtFoam released by F. Ettner [17,24]. The code is based on an open-source freeware OPENFoam software. The main advantage of ddtFoam is its capability to capture the flame acceleration process together with the transition to detonation based on the dual-source term in the reaction progress transport equation. First term responsible for the deflagration is based on the Weller [25] gradient combustion model, while the second term accounts for autoignition delay time. The second term is especially important as the autoignition delay time is a function of local conditions of temperature, pressure, and mixture composition. To prevent calculating ignition delay time in every time step and computational cell, the solver is using pre-calculated table of ignition delay time (IDT) prepared with Cantera software with detailed reaction mechanism of O'Conaire [26]. The IDT table is accessed during the simulation and the solver compares the tabulated IDT (as a function of temperature, pressure, and composition) with the simulated fluid residence time at specific conditions. If the residence time excess the precalculated IDT value, the solver activates the second source term in the reaction progress transport equation. Such an approach significantly reduces the numerical cost of simulation. Similarly, the combustion products matrix as a function of the initial temperature, pressure, and composition is precalculated and accessed while the simulation progresses. Some memory saving modification for this methodology using a multiple regression model was introduced and tested in the recent paper of Malik et al. [27]. An additional advantage of ddtFoam is the presence of a shock wave sub-grid model to better capture the progress of the shock wave induced temperature rise within a single cell. The computational cell in this model is virtually divided into shocked and non-shocked volumes and IDT is evaluated for both volumes. Such a combination leads to greater accuracy of the results at course grids. Up to date, the ddtFoam has been used to investigate the DDT process in mixtures with hydrogen concentration gradients, large scale experiments with and without adaptive mesh refinement [28], smooth channels with mixtures of hydrogen-oxygen [27], and channels with obstacles [29].

One of the first papers by Ettner [17] described the code together with the test 2D simulations of the flame propagating in hydrogen–air mixture with concentration gradient in the channel with a variety of blockage ratios. The results showed good agreement with experiments by means of the velocity profile along the channel and pressures recorded. Additionally, the code was able to capture phenomena recorded in experiments and highly resolved simulations like Mach stem formation, DDT due to the shock wave reflection,

and shock–flame interaction. Another important conclusion was that the rectangular grids finer than 2 mm did not affect the results apart from the pressure peaks sharpness in stable detonation mode. Such ddtFoam code advantage arises from the IDT and shock-wave sub-models implemented and let one use it in large-scale geometries with relatively coarse grids.

Hasslberger et al. [28] used ddtFoam to simulate a large-scale RUT facility [23] at the hydrogen concentration close to the lower detonability limit. The approach was to use a 3D domain with adaptive mesh refinement at the flame surface to increase accuracy and decrease the computational cost. Two experiments were simulated with very good agreement with respect to flame acceleration. The first experiment (14% H_2) was well-predicted with respect to the detonation transition placement at the reflecting surface. The second experiment (12.5% H_2) simulation did not provide a successful transition, however, the experimental detonation origin was reported [23] to be in the flame brush area rather than due to the shock wave reflection at the wall.

The main purpose of the ddtFoam design was to address the fact that large-scale accidents simulations must be performed under resolved grids. Therefore, the sub-grid modeling of critical phenomena is necessary to provide sufficient accuracy and minimize the computational time of the simulation. Critical for DDT process phenomena recognized by Ettner [17] were shock wave reflection and triggering conditions for a successful transition to detonation. Both were addressed by sub-grid modeling described earlier in this chapter. As sub-grid modeling demands validation for a variety of scales the present work might be considered as a next step to validate the code with experimental data and point at possible, further improvements. The main aim of this study was to assess the capabilities of ddtFoam code to capture the limits of hydrogen in the air for which successful transition to detonation might be observed. The numerical results are compared to the experimentally recorded values measured for three different obstacle spacing configurations with a fixed blockage ratio of 0.5. The comparison was made for such parameters as pressure profiles, maximum overpressures, run-up distance, and DDT limits.

2. Experimental Setup Description and Results

The experimental setup has been previously used for the investigation of the scale effect of the obstacle-filled 2-m-long channel and the results are reported in the paper of Teodorczyk [30]. The current setup has been extended to 4 m to observe further flame acceleration, the transition to detonation, and stable detonation. The tube consisted of two 2-m-long sections with dimensions of 0.08 × 0.11 m in cross-section (H × W). The obstacles were made of aluminum 10 mm thick and 40 mm high, which provided a constant blockage ratio of 0.5 for all obstacles spacing configurations. The spacing S between obstacles was equal to H, 2H, 3H. Initial conditions for the H_2–air mixture were T = 295 ± 3K and P = 0.1 MPa. The hydrogen concentration in air was within 15–55% [vol./vol.], which corresponds to an equivalence ratio of 0.42–2.92. The total number of experiments was nearly 300. The number of experiments for each mixture composition and geometrical configuration was 10–13 for most of the tests, three configurations were tested with 4, 5, or 7 single experiments. The weak ignition source was a spark plug placed at one end of the channel at its half-height middle-width. The measurements included 8 PCB 113B24 type pressure sensors (PS1–PS8) with a measurement range of 6.7 MPa and 8 in-house made ion probes (IP1–IP8). Sensors were placed in pairs along the tube to indicate pressure wave and the following flame. Velocity profile was measured based on the time-of-arrival method (ToA). The scheme of the experimental setup is presented in Figure 1. The tube cross-section for all obstacles spacing considered is presented in Figure 2. An example graph of the pressure sensors and ion probes profiles is presented in Figure 3 in which each of 8 colors corresponds to a consecutive set of sensors. The same color scheme applies to pressure profiles presented in this paper. The clearly visible largest delay between signals from PS5 and PS6 is due to the most distant (893 mm) placement between both sensors. More detailed experimental setup description is available in References [30,31].

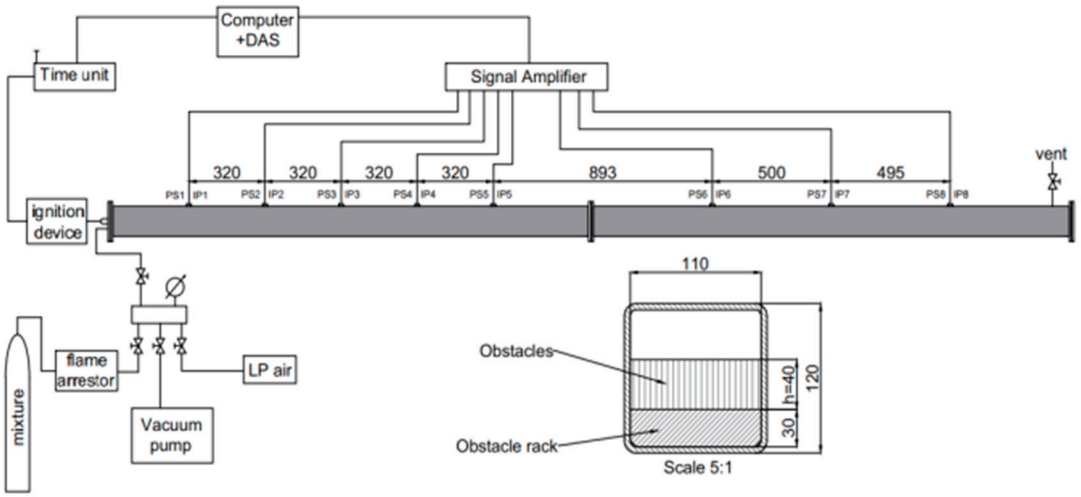

Figure 1. Experimental setup scheme. Setup used for measurements of deflagration to detonation transition process (DDT) limits in H_2–air mixtures [31]. Distance between pairs of sensors in mm.

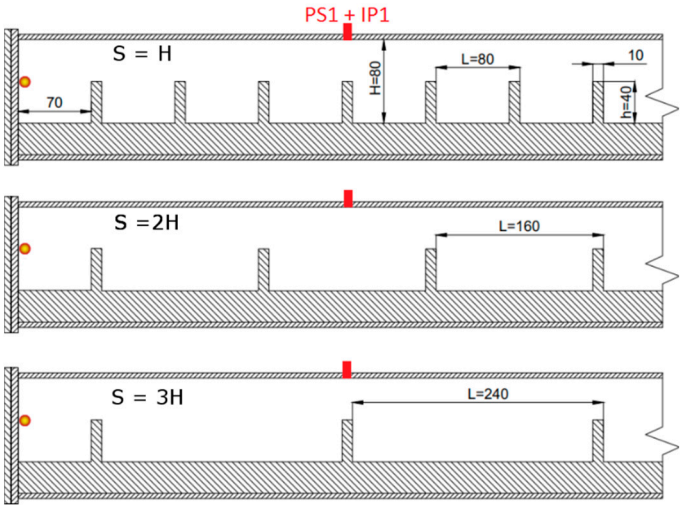

Figure 2. Detonation tube cross-section for different obstacles spacings. Orange point marks the ignition point position, red rectangle marks first pair of sensors placement: pressure sensor (PS1) and ion probe (IP1); both sensors at 320 mm axial distance from the ignition point.

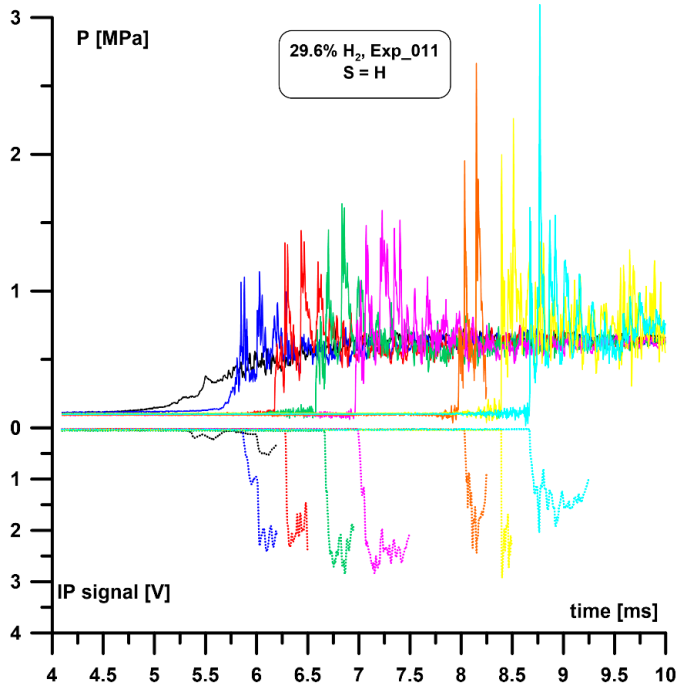

Figure 3. Experimental pressure sensors and ion probes profiles for 29.6% H_2 in air (φ = 1.0) case S = H. Sequence of sensors activation corresponds to the order of sensors position as in Figure 1. Same colors apply to pressure sensors (top) and ion probes (bottom) at the same position.

The main results of the experimental research [31] are summarized in Table 1 and in Figure 4 with DDT limits for all spacings and with the mean velocities measured at the end of the detonation tube. The assumption was that the mixture is within the DDT limits if at least one test proved transition to detonation in any of the repeated experimental sets. The limits of DDT were, therefore, extreme mixtures for such experimental sets. What is clear from Figure 4 that with the obstacles spacing increase the DDT limits get wider and simultaneously mean detonation velocities increase.

Table 1. DDT limits observed experimentally in 4-m long tube [30,31].

DDT Limits	S = H	S = 2H	S = 3H
% H_2 in air	27.4–38.6	25.0–50.0	20.0–50.0

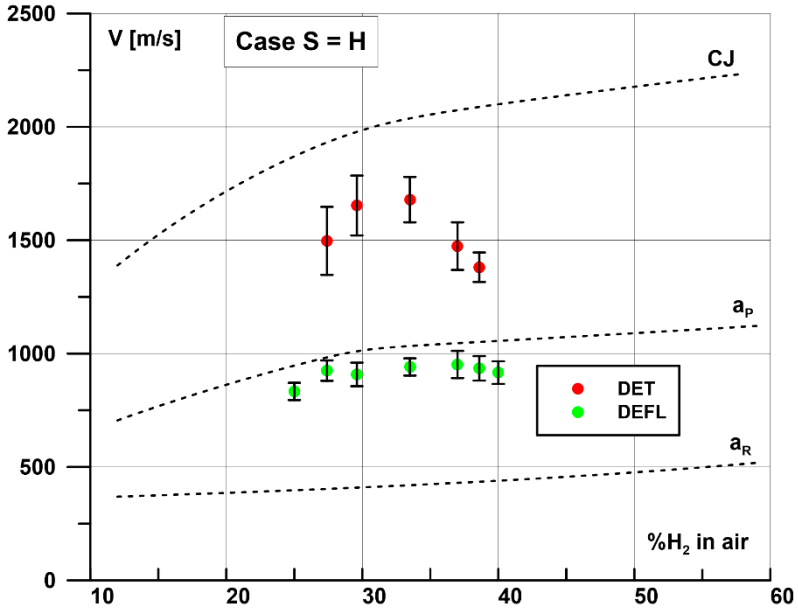

(**a**)

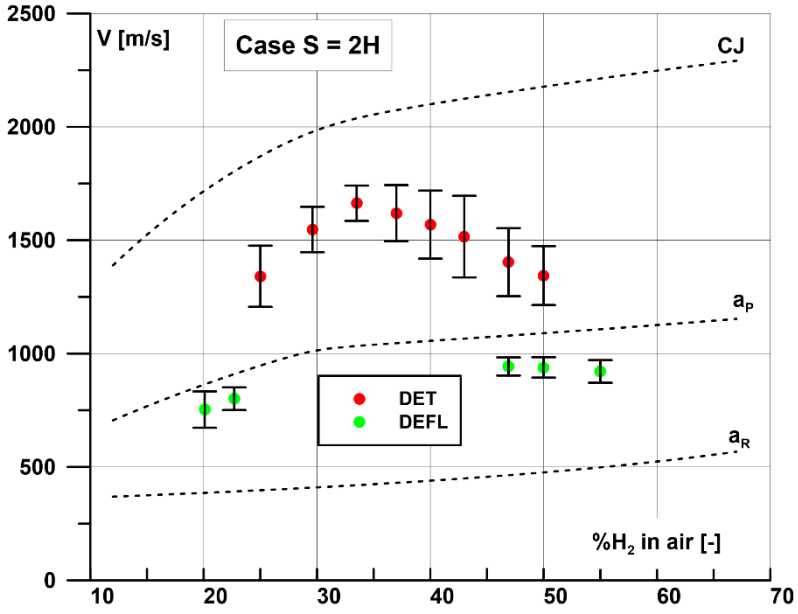

(**b**)

Figure 4. *Cont.*

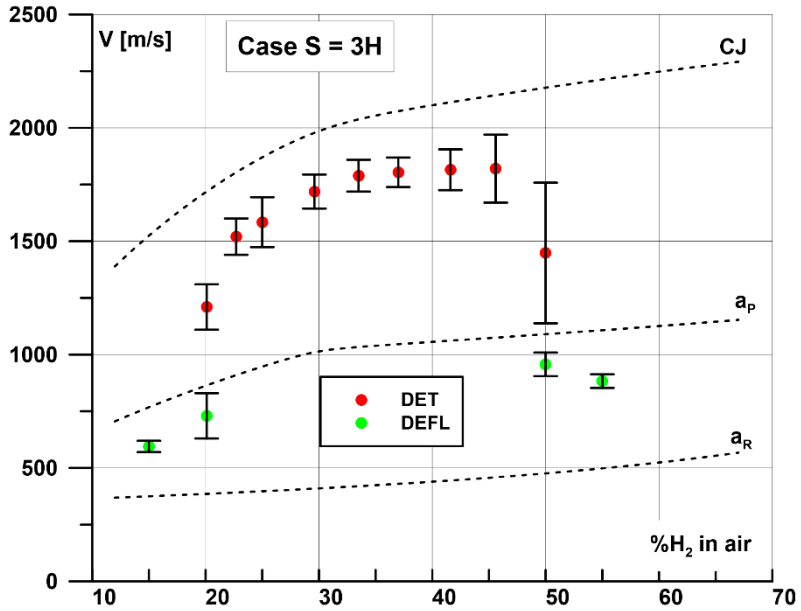

(**c**)

Figure 4. Mean velocities recorder for deflagration experiments (green dots) and experiments with DDT (red dots) for three obstacles configurations: (**a**) S = H, (**b**) S = 2H, (**c**) S = 3H [31]. CJ—Chapman Jouguet detonation velocity, a_P—speed of sound in products, a_r—speed of sound in reactants. Whiskers correspond to the minimum and maximum velocities recorded within the mixture investigated. DET—case with successful transition to detonation, DEFL—case with deflagration only.

3. Numerical Simulations Description

Numerical simulations were performed with the use of ddtFoam code initially described in the Introduction chapter. The ddfFoam solves the unsteady and compressible Navier-Stokes equations density-based. Harten, Lax and van Leer (HLLC) Riemann scheme [32] is used to solve convective terms with multidimensional slope limiters [33,34] suitable for compressible high Mach number. More details of the numerical code schemes can be found in References [17,24,33]. The numerical domain was 2D representing the longitudinal cross-section of the experimental detonation tube channel. The numerical channel was, therefore, 4 m in length and 0.080 m in height. The numerical mesh was orthogonal and structural and contained approximately 320,000 cells, 1 mm by 1 mm each. In total, 36 simulations were performed for various hydrogen in air concentrations in the range of 15–65% H_2 in air, which corresponds to equivalence ratio 0.42–4.42. Initial temperature and pressure were set to 293 K and 101,325 Pa, respectively. The walls were considered as non-slip and adiabatic. The numerical ignition spot was in a form of 25 mm radius area patch filled in with hot combustion products. The center of the ignition spot was at the same position as in experiments, at the center of the channel height at one end of the tube. During the simulations, temperature and pressure numerical sensors were placed at the same position as in experiments. The pre-calculated table of ignition delay time was prepared based on the detailed reaction mechanism of O'Conaire [26] and Cantera software calculations [35]. For turbulence modeling, k-omega SST (Shear Stress Transport) turbulence model has been chosen. This modeling approach combines the advantages of k-ε and k-ω as in regions near walls it behaves like k-ω and switches to k-ε in a free stream region. Wall function utilized was OPENFOAM built-in function KqRWallFunction and omegaWallFunction appropriate for high re-flows. Turbulent kinetic energy k and specific dissipation rate ω were initialized according to Ettner's settings [17]. The time step of the simulation was adaptive according to Courant-Friedlich-Lewy (CFL) condition at the maximum possible value of 0.5. The simulation time of a single case was around 70 h on a 28 CPU workstation.

4. Results

The numerical results were postprocessed in a similar way as in experiments by recording pressure sensors indications (via ToA method) and extracting velocity profiles of the shock wave along the tube. Further postprocessing was done by extracting contour diagrams of pressures and temperature along the channel, which indicated the placement of the transition to detonation that defined the numerical detonation run-up distance (RUD). Typical contours of pressure and temperature during the transition to detonation process are presented in Figure 5.

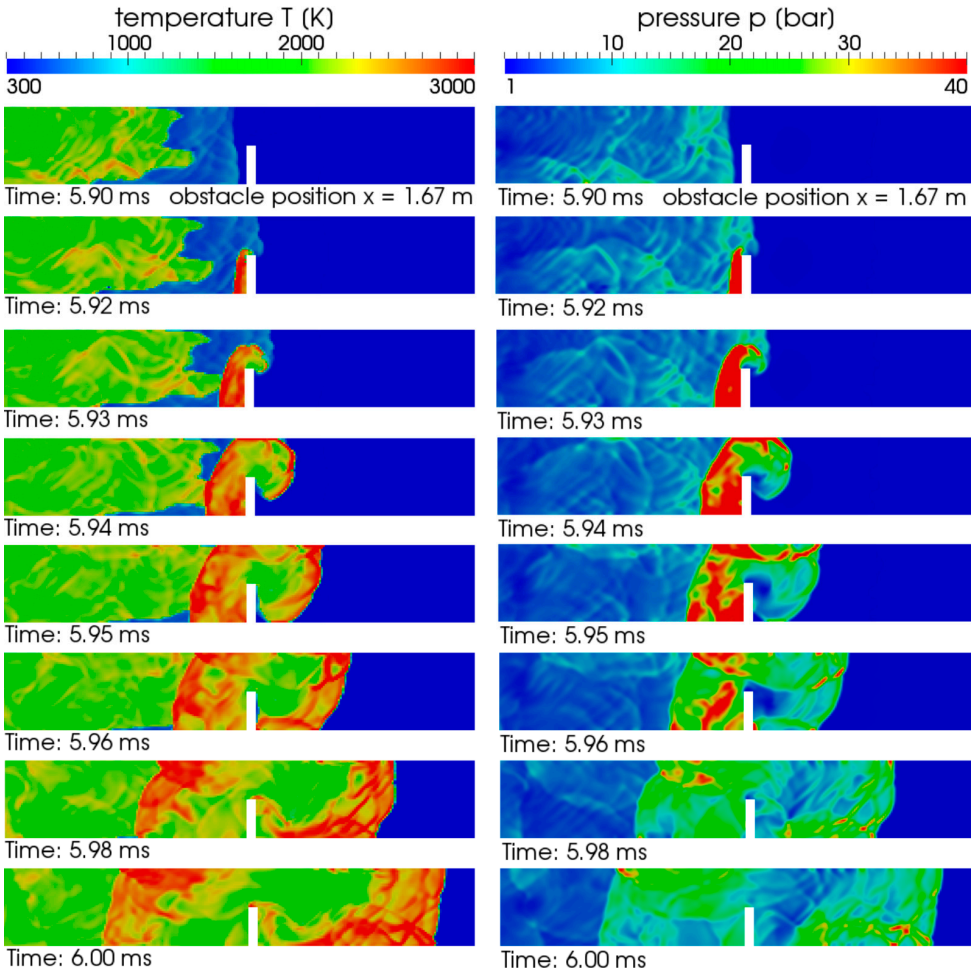

Figure 5. Transition to detonation due to the shock wave reflection at the obstacle for case 50% H_2 and S = 3H.

The following sections describe the obtained numerical results divided with respect to the spacing between obstacles. The comparison included selected pressure profiles, flame velocities, and run-up distances.

4.1. Case S = H

For this geometry, 10 simulations were performed with 15–55% H_2 in air. The sample experimental and numerical pressure profiles with deflagration along the channel are presented in Figure 6. The simulation time has been shifted to make an easier comparison between corresponding sensors. The reason for the time difference was mainly due to the specific spark release system used which was not always activated at the same time as the data acquisition system. In Figure 6, one can observe that corresponding numerical and experimental pressure profiles are very similar especially for sensors placed at the further part of the tube where the mixture burns in a fast deflagration regime. The leading

shock wave preceding the larger pressure peak at the flame front might also be visible there. Further pressure oscillations are due to the shock wave reflections propagating in the post-combustion products. In the case of the first part of the tube where flame accelerates, the match between simulation and experiment is less visible. This suggests further numerical investigation and testing of the combustion model that works in a slow deflagration regime of combustion. Figure 7 shows a comparison between pressure profiles showing stable detonation. In this case, both, numerical and experimental detonation front peak pressures, are within the range of 2–2.5 MPa. However, in some experiments, peak pressures reached 3.5–4.0 MPa. Figure 8 shows the velocities measured for all considered simulations in case S = H together with experimental values. Based on that graph, one can distinguish numerical cases with and without DDT. It can be derived that for case S = H, the numerical DDT limits are of 20% and 50% of hydrogen in air. The postprocessed simulations and experimental data were further used to define the RUD profile. In the case of experiments, the RUD was defined as the distance from the ignition point to the first sensor, which recorded detonation. As the exact place for the transition to detonation might happen at a slightly shorter distance, the RUD graphs are equipped with negative whiskers covering the distance to the previous sensor. In the case of simulations, the run-up distance was defined as the distance to the point where the transition to detonation took place. The comparison between experimental and numerical RUD is presented in Figure 9. One can notice that numerical RUD values are much shorter than experimental, and the curve has a characteristic U-shape. For the stoichiometric mixture, the ratio of numerical to experimental RUD is close to 2. However, one needs to bear in mind that in the case of S = H, the significant velocity deficit is observed due to the cyclic detonation attenuation and re-initialization type of propagation, so-called quasi-detonation. Therefore, it cannot be ruled out that in experiments, the detonation was initiated and extinguished shortly after, and sensors did not record it.

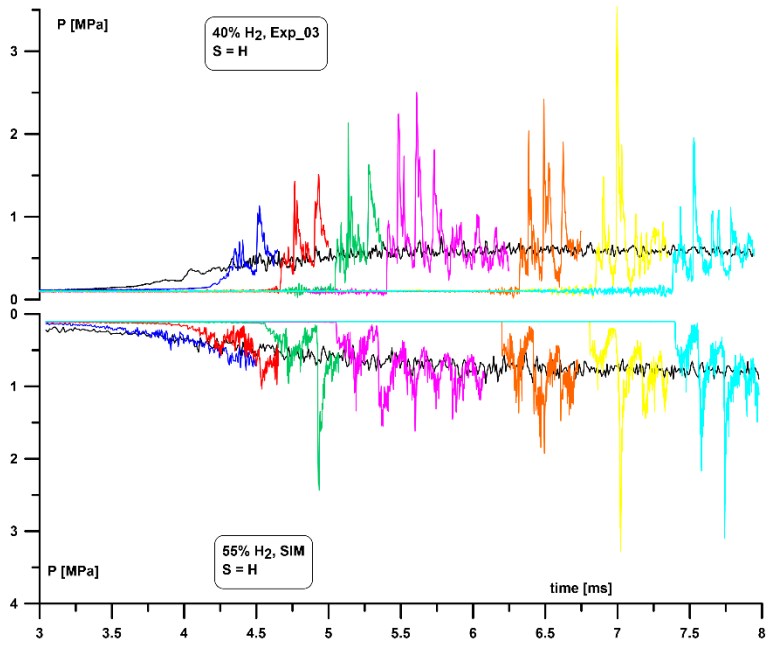

Figure 6. Experimental (top) and numerical (bottom) pressure profiles with deflagration for case S = H. Sequence of sensors activation corresponds to the sensors position as in Figure 1. Same colors apply to sensors in the same position. Simulation time shifted +2.5 ms for better visibility.

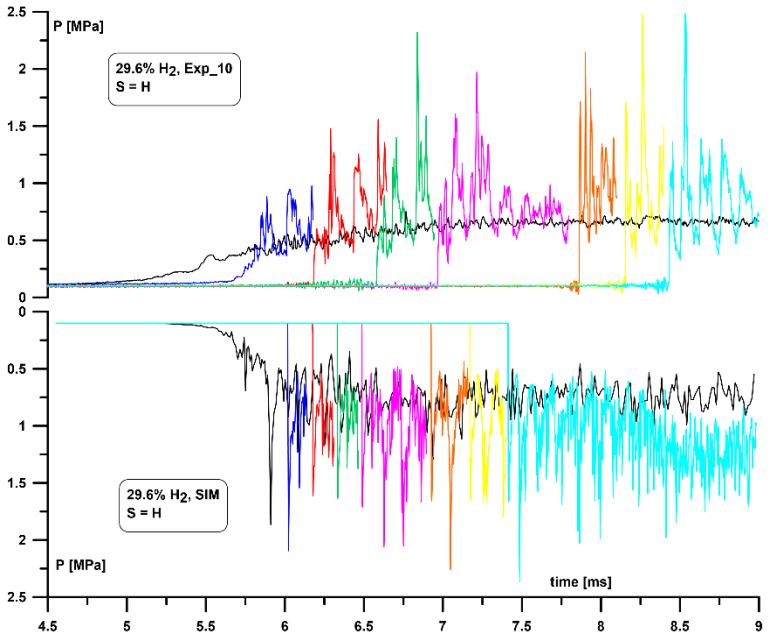

Figure 7. Experimental (top) and numerical (bottom) pressure profiles with detonation for case S = H and 29.6% H_2 in air. Sequence of sensors activation corresponds to the sensors position as in Figure 1. Same colors apply to sensors in the same position. Simulation time shifted +4.3 ms for better visibility.

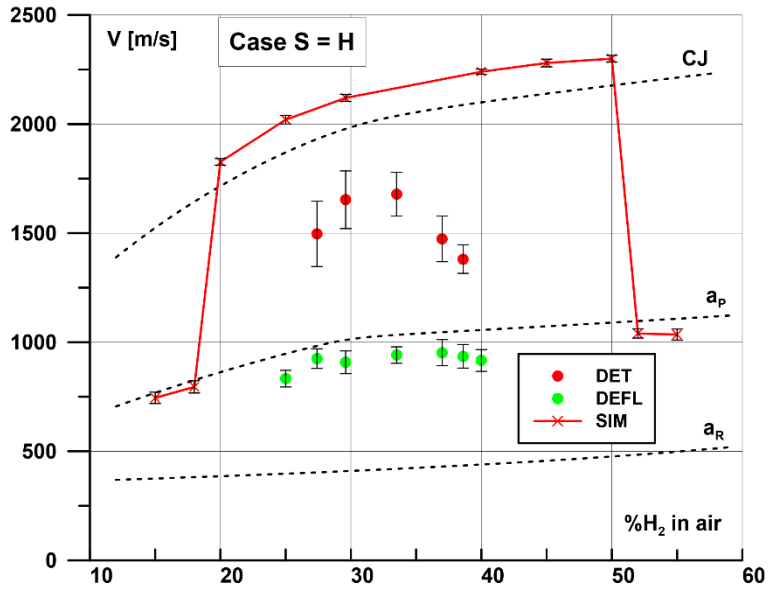

Figure 8. Propagation velocity as a function of mixture composition for S = H. Simulation results (line) and experimental results (dots) [31].

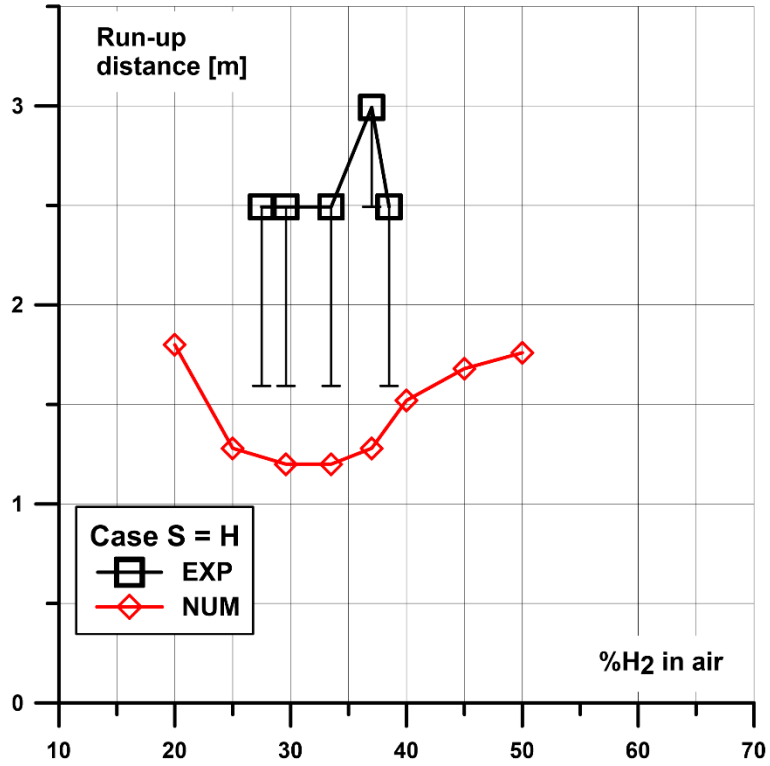

Figure 9. Run-up distances for S = H spacing geometry. Experimental data whiskers cover the distance range of possible transition to detonation placement.

4.2. Case S = 2H

For this geometry, 13 simulations were performed for 15–67% of H_2 in air. The sample pressure profile along the channel for simulation and experiment with DDT for 29.6% H_2 in air (φ = 1.0) is presented in Figure 10. One can see that the transition to detonation took place between 4th (1.28 m from ignition) and 5th (1.6 m from ignition) pressure sensor while in the simulation it was very close to the 3rd sensor (0.96 m from ignition). In both cases, the transition to detonation was recorded with high pressure peak reaching 5 MPa in simulation and 4.5 MPa in the experiment. Such peak is very often observed in experiments in which the sensor is close enough to the hot spot where initial, locally overdriven detonation is generated. Further sensors indications are very similar for both, simulation and experiments and pressure peaks, are within 1.5–2.3 MPa range. Figure 11 shows the sample pressure profiles of the simulation and experiment with deflagration. In the experiment, one can see the leading shock wave preceding the flame front pressure peak similar to in case S = H. The shock wave in the experiment is generated before 4th sensor (0.96 m from ignition), while a similar shock wave is visible in simulation around the 6th sensor (2.49 m from ignition). Similarly, as in the previous case, the slow deflagration pressure profiles are not represented in simulations as well as the fast deflagration. Figure 12 presents a comparison of velocities measured in experiments and simulations. Based on that graph, one may define the numerical DDT limits for S = 2H, which are very close to 18% and 62.5% of H_2 in air. The experimental and numerical RUD is presented in Figure 13. Similar to in case S = H, the numerical RUD curve for S = 2H is U-shaped, however, the experimental RUD seems to be closer to the numerical one with a value of around 1.5 m for near stoichiometric composition. Similarly, as in S = H, we cannot exclude that the detonation took place earlier, but the limited number of sensors did not allow us to record the exact place of that process.

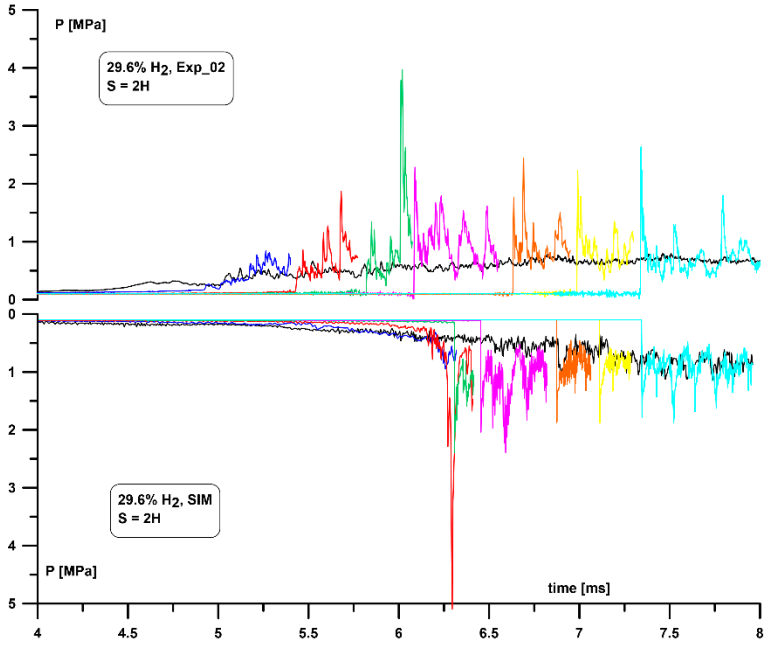

Figure 10. Experimental (top) and numerical (bottom) pressure profile with detonation for case S = 2H and 29.6% H_2 in air. The sequence of sensor activation corresponds to the sensors position as in Figure 1. Same colors apply to sensors in the same position. Simulation time shifted +1 ms for better visibility.

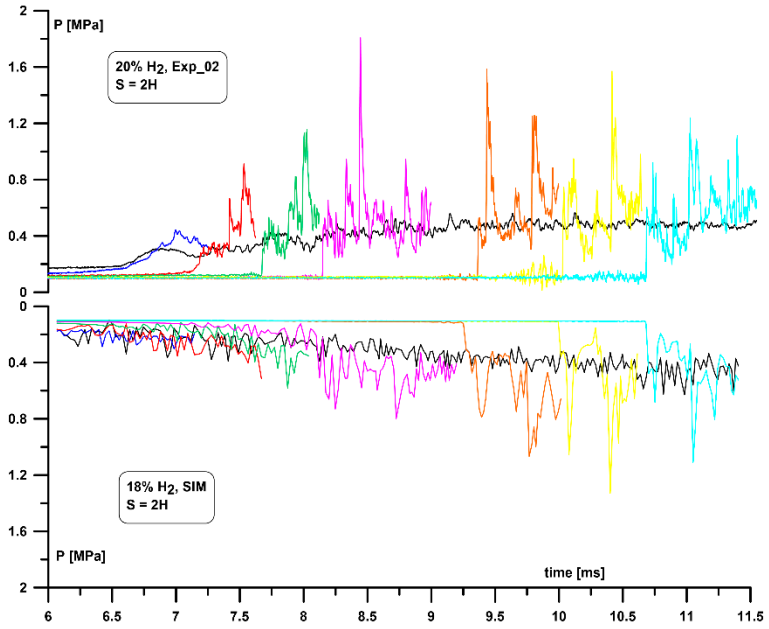

Figure 11. Experimental (top) and numerical (bottom) pressure profiles with deflagration for case S = 2H. Sequence of sensors activation corresponds to the sensors position as in Figure 1. Same colors apply to sensors in the same position. Simulation time shifted +5.5 ms for better visibility.

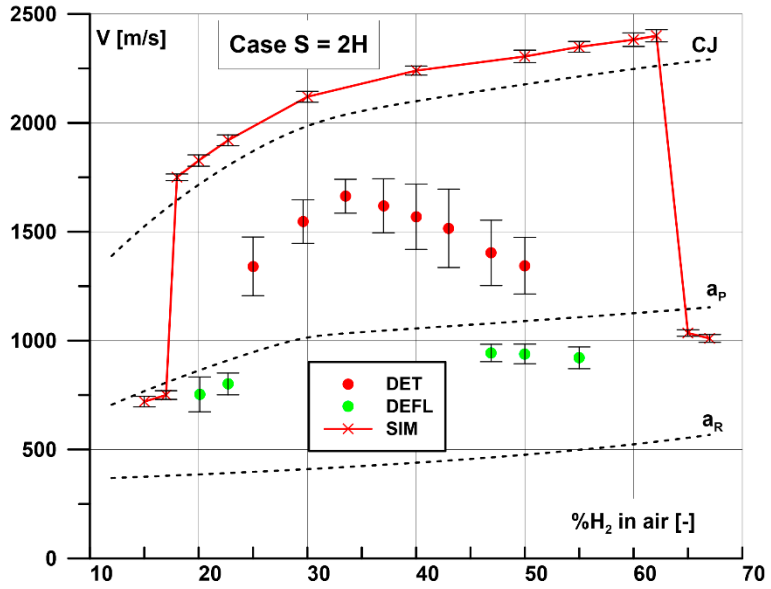

Figure 12. Propagation velocity as a function of mixture composition for S = 2H. Simulation results (line) and experimental results (dots) [31].

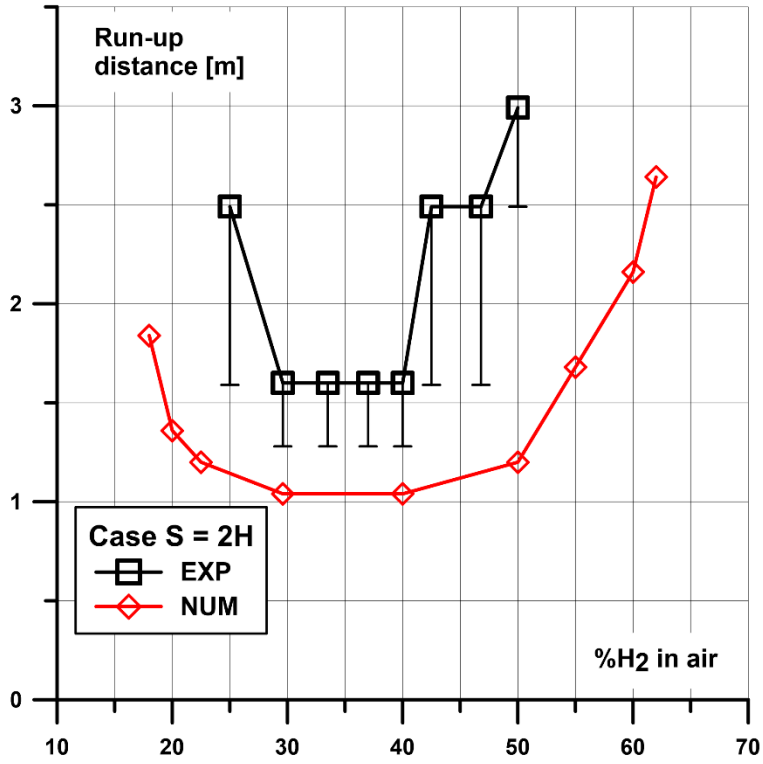

Figure 13. Run-up distances for S = 2H spacing geometry. Experimental data whiskers cover the distance range of possible transition to detonation placement.

4.3. Case S = 3H

For this geometry, 12 simulations were performed for 15–65% H_2 in air. The sample pressure profile along the channel for simulation and experiment with a detonation in mixture 29.6% H_2 in the air is presented in Figure 14. Transition to detonation in the experiment took place between 4th (1.28 m from ignition) and 5th (1.6 m from ignition) sensor while in the simulation it was very close to the 3rd sensor (0.96 m from ignition). In both cases, the transition to detonation was recorded with high pressure peak reaching

3.5 MPa. Further sensors indications of detonation front are similar for both, simulation and experiments and pressure peaks, are within 1.8–2.5 MPa range. Similarly, as in case S = H and S = 2H, the simulations underpredict overpressures for slow deflagration. Figure 15 shows a comparison between experimental and numerical cases with deflagration. Numerical pressure profiles for the initial stage of flame propagation (first five sensors) do differ compared to the experiments; however, the maximum overpressures seem to be consistent. Further pressure profiles (last three sensors) match better with experimental ones by means of the overpressure values and shape. In simulations, however, the further pressure peaks due to the shock wave reflections from the walls are not so apparent. Figure 16 shows a comparison of velocities measured in experiments and simulations. Based on that graph, one may define the numerical DDT limits for S = 3H, which are very close to 18% and 55% of H_2 in air. The experimental and numerical RUD is presented in Figure 17. Similar to in case S = H and S = 2H, the numerical RUD curve for S = 3H is U-shape type with a minimum between 30–40% H_2, which means that for less reactive mixtures, the flame needs to propagate further to provide sufficient conditions to generate hot spots and stable detonation front.

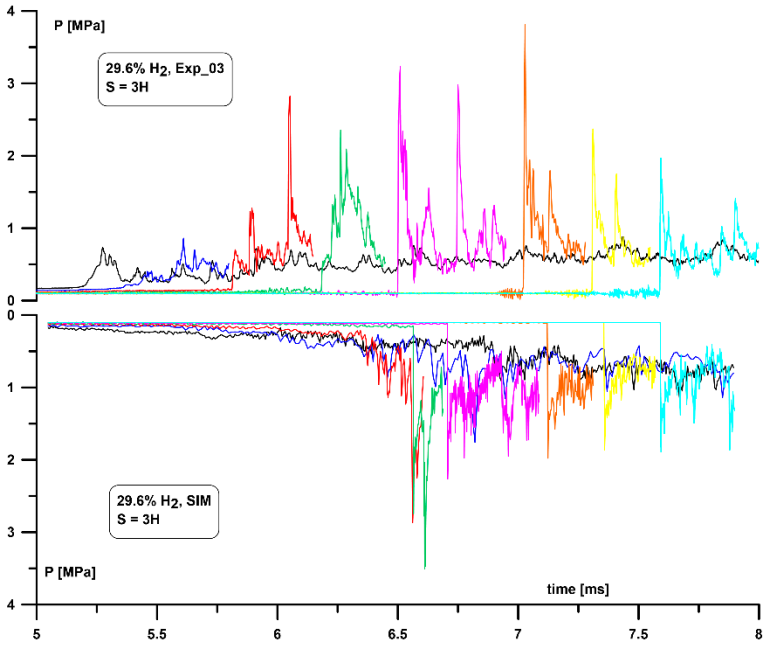

Figure 14. Experimental (**top**) and numerical (**bottom**) pressure profile with detonation for case S = 3H and 29.6% H_2 in air. Sequence of sensors activation corresponds to the sensors position as in Figure 1. Same colors apply to sensors in the same position. Simulation time shifted −1.0 ms for better visibility.

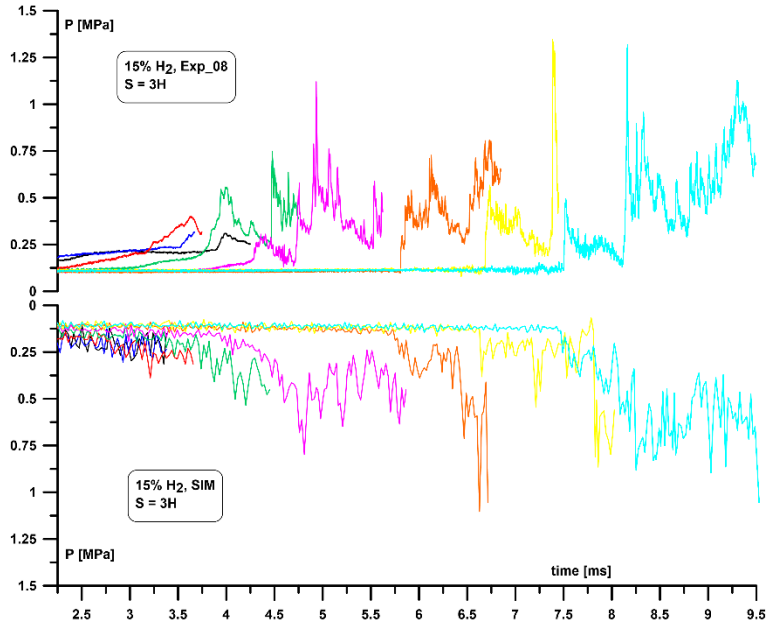

Figure 15. Experimental (**top**) and numerical (**bottom**) pressure profile with deflagration for case S = 3H and 15% H_2 in air. Sequence of sensors activation corresponds to the sensors position as in Figure 1. Same colors apply to sensors in the same position. Simulation time shifted −5 ms for better visibility.

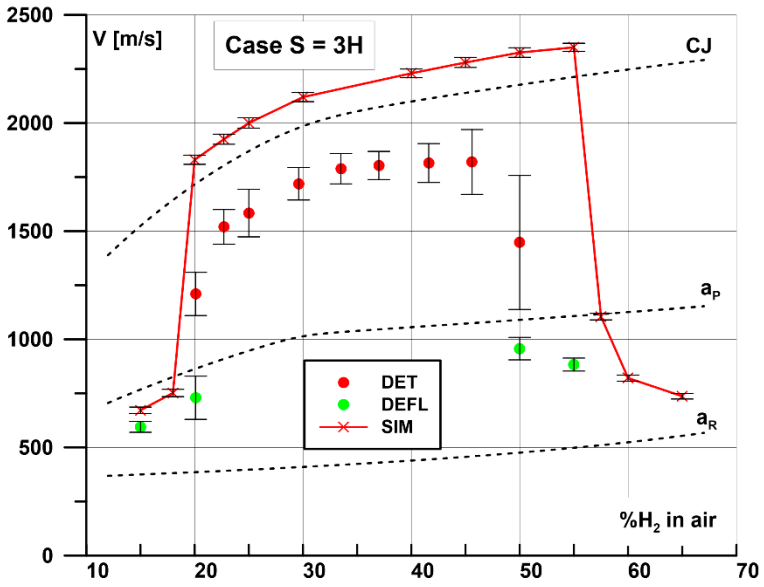

Figure 16. Propagation velocity as a function of mixture composition for S = 3H. Simulation results (line) and experimental results (dots) [31].

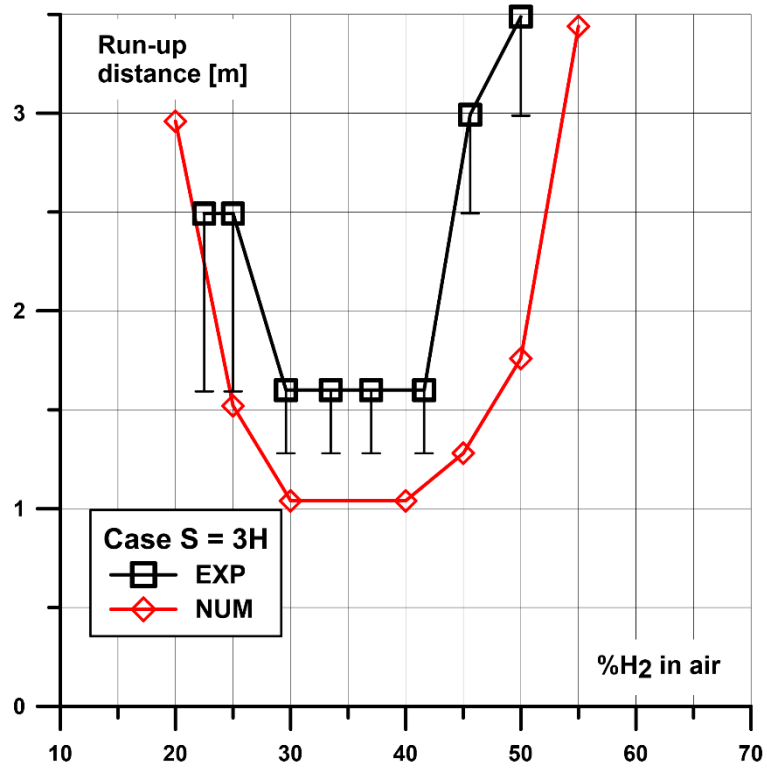

Figure 17. Run-up distances for S = 3H spacing geometry. Experimental data whiskers cover the distance range of possible transition to detonation placement.

5. Discussion

The numerical and experimental DDT limits values are summarized in Table 2. The lower DDT limits obtained numerically are very similar for all considered geometries and very close to 20% H_2 in air. The upper DDT limits in simulations differ and are in the range of 50–62.5% H_2 depending on the obstacle spacing. The best match between experimental and numerical limits is for case S = 3H, which is also confirmed by means of the RUD comparison (see Figure 17). The maximum overpressures recorded were also similar and within 1.8–2.5 MPa range for both, experiments and simulations, in case S = 3H. The worst match is observed for case S = H. This effect might be explained by means of the cyclic initiation and attenuation of real detonation front in a more congested configuration. This type of cyclic process called quasi-detonation is a result of more dense congestion, which leads to higher momentum losses, diffraction of the detonation wave behind the obstacle, and, therefore, lower mean detonation velocity observed in experiments comparing to the ideal C-J velocity.

Table 2. DDT limits measured experimentally [31] and obtained numerically (this work).

DDT Limits	S = H		S = 2H		S = 3H	
	Exp.	Num.	Exp.	Num.	Exp.	Num.
Lower limit [% H_2]	27.4	20	25	18.0	22.7	20
Upper limit [% H_2]	38.6	50	50	62.5	50	55

Simultaneously, such detonation behavior is not observed in numerical simulations as the implemented adiabatic flow model is less sensitive to the heat and momentum losses, which are of importance in real reactive flow. Additionally, simulations do not include some effects of the channel geometry (for lower obstacles spacing) on initiation, cellular structure development, and further stable propagation or attenuation of detonation. In the case of lower obstacles spacing, the interaction of obstacles on real 3-dimensional

detonation front structure is the strongest, which has been confirmed by experiments. In less congested geometries, the detonation is more prone to develop and propagate stably, which is expressed by higher mean experimental velocities and wider DDT limits. Simultaneously, in less congested geometries, the transition to detonation was observed due to the reflection at the obstacles surface [31], which is the main mechanism triggering detonation in simulations. Due to that fact one might conclude that ddtFoam is more suitable to simulate geometries with a relatively low level of congestion and for more congested geometries the code will provide conservative results with some safety margin. Considering the flame acceleration process, pressure profiles, and overpressure values along the congested channel, it must be concluded that these parameters are well represented for all the considered geometrical configurations, especially for the fast deflagration propagation regime. RUDs are numerically predicted as a U-shaped curve with the best match to the experimental curve for S = 3H configuration. Discrepancies might be observed in stable detonation front velocity, which is overpredicted with respect to ideal C-J detonation, and the change between deflagration and detonation regime of combustion is very sharp. These features arise from the implemented specific autoignition model. The main 'trigger' to switch simulation to detonation is the sufficiently low ignition delay time. Therefore, numerical detonation once initiated will propagate if the unburned mixture will be available independently on the channel blockage ratio. This code feature does not seem to be critical as properly predicted flame acceleration process together with overpressures and RUD are of greater importance. The ddtFoam code is not equipped with a numerical mechanism attenuating initially stable detonation, as a result, the numerical quasi-detonation process is not possible to be observed. This fact is especially visible in comparison between experimental and numerical results for case S = H. That code feature might be one of the future code improvement subjects. Additionally, the numerical model is not able to predict cellular detonation front structure; therefore, it omits all the effects arising from this characteristic detonation dimension. This feature might be also a subject for further code development.

6. Conclusions

The main aim of this work was to perform numerical simulations of the DDT process and assess the ddtFoam code capabilities to predict DDT limits observed in experiments in an obstacle-laden tube. Three different geometrical configurations have been considered which correspond to the experimental setup: S = H, 2H, 3H. The numerical DDT limits were wider than experimental with the largest discrepancies observed for the lowest spacing S = H. Such feature is expected as walls in simulations were considered as adiabatic and did not include heat and momentum losses effects caused by more congested channels. In more congested channels, so-called quasi-detonation was observed in experiments, which was expressed by significantly lower than ideal C-J mean detonation velocity along the channel. Additionally, in experiments for S = H within the DDT limits, detonation was not always observed (green points in Figure 4). This witness the randomness of the real DDT process itself, especially in more congested geometry. The results of the simulations together with the discussed ddtFoam code features point at its main possible application as a robust, engineering tool for hydrogen–air DDT process simulation in geometries with a relatively low level of congestion. As the presented work indicates, simulations in such geometries provide close to experimental results with respect to flame acceleration velocity profiles, run-up distance, and overpressures.

Author Contributions: Conceptualization, W.R. and A.T.; data curation, W.R.; formal analysis, W.R.; investigation, W.R.; methodology, W.R.; project administration, W.R.; resources, W.R.; software, W.R.; supervision, A.T.; validation, W.R.; visualization, W.R.; writing—original draft, W.R.; writing—review and editing, A.T. Both authors have read and agreed to the published version of the manuscript.

Funding: This experimental research presented in this paper was funded by the Dean of Faculty of Power and Aeronautical Engineering, grant number 504/03263/1131/42.

Data Availability Statement: The data presented in this study are available on request from the corresponding author.

Acknowledgments: The authors would like to acknowledge the Dean of Faculty of Power and Aeronautical Engineering for financial support and the Interdisciplinary Centre for Mathematical Computational Modelling (ICM), the University of Warsaw, for sharing HPC computational resources within the grant no. G71-17.

Conflicts of Interest: The authors declare no conflict of interest.

References

1. Dorofeev, S.B.; Sidorov, V.P.; Kuznetsov, M.S.; Matsukov, I.D.; Alekseev, V.I. Effect of scale on the onset of detonations. *Shock Waves* **2000**, *10*, 137–149. [CrossRef]
2. Dorofeev, S.B.; Kuznetsov, M.S.; Alekseev, V.I.; Efimenko, A.A.; Breitung, W. Evaluation of limits for effective flame acceleration in hydrogen mixtures. *J. Loss Prev. Process. Ind.* **2001**, *14*, 583–589. [CrossRef]
3. Kellenberger, M.; Ciccarelli, G. Advancements on the propagation mechanism of a detonation wave in an obstructed channel. *Combust. Flame* **2018**, *191*, 195–209. [CrossRef]
4. Cross, M.; Ciccarelli, G. DDT and detonation propagation limits in an obstacle filled tube. *J. Loss Prev. Process. Ind.* **2015**, *36*, 380–386. [CrossRef]
5. Li, Q.; Kellenberger, M.; Ciccarelli, G. Geometric influence on the propagation of the quasi-detonations in a stoichiometric H_2-O_2 mixture. *Fuel* **2020**, *269*, 117396. [CrossRef]
6. Teodorczyk, A.; Lee, J.H.S.; Knystautas, R. Propagation mechanism of quasi-detonations. *Symp. Combust.* **1989**, *22*, 1723–1731. [CrossRef]
7. Teodorczyk, A. Fast deflagrations, deflagration to detonation transition (DDT) and direct detonation initiation in hydrogen-air mixtures. *First Eur. Summer Sch. Hydrog. Saf.* **2006**, *2*, 15–24.
8. Rudy, W.; Kuznetsov, M.; Porowski, R.; Teodorczyk, A.; Grune, J.; Sempert, K. Critical conditions of hydrogen-air detonation in partially confined geometry. *Proc. Combust. Inst.* **2013**, *34*, 1965–1972. [CrossRef]
9. Kuznetsov, M.S.; Alekseev, V.I.; Dorofeev, S.B. Comparison of critical conditions for DDT in regular and irregular cellular detonation systems. *Shock Waves* **2000**, *10*, 217–223. [CrossRef]
10. Kuznetsov, M.; Ciccarelli, G.; Dorofeev, S.; Alekseev, V.; Yankin, Y.; Kim, T.H. DDT in methane-air mixtures. *Shock Waves* **2002**, *12*, 215–220. [CrossRef]
11. Kogarko, S.M.; Zeldovich, Y.B. Doklad. Doklady Akademii Nauk SSSR NS63. 1948. Available online: https://catalyst.library.jhu.edu/catalog/bib_2560400 (accessed on 1 September 2020).
12. Rudy, W.; Dziubanii, K.; Zbikowski, M.; Teodorczyk, A. Experimental determination of critical conditions for hydrogen-air detonation propagation in partially confined geometry. *Int. J. Hydrog. Energy* **2017**, *42*, 7366–7373. [CrossRef]
13. Rudy, W.; Zbikowski, M.; Teodorczyk, A. Detonations in hydrogen-methane-air mixtures in semi confined flat channels. *Energy* **2016**, *116*, 1479–1483. [CrossRef]
14. Khokhlov, A.M.; Oran, E.S.; Thomas, G.O. Numerical simulation of deflagration-to-detonation transition: The role of shock-flame interactions in turbulent flames. *Combust. Flame* **1999**, *117*, 323–339. [CrossRef]
15. Gamezo, V.N.; Ogawa, T.; Oran, E.S. Deflagration-to-detonation transition in H_2-air mixtures: Effect of blockage ratio. In Proceedings of the 47th AIAA Aerospace Sciences Meeting including The New Horizons Forum and Aerospace Exposition, Orlando, FL, USA, 5–8 January 2009; p. 440.
16. Boeck, L.R.; Hasslberger, J.; Sattelmayer, T. Flame Acceleration in Hydrogen/Air Mixtures with Concentration Gradients. *Combust. Sci. Technol.* **2014**, *186*, 1650–1661. [CrossRef]
17. Ettner, F.; Vollmer, K.G.; Sattelmayer, T. Numerical Simulation of the Deflagration-to-Detonation Transition in Inhomogeneous Mixtures. *J. Combust.* **2014**, *2014*, 1–14. [CrossRef]
18. Ettner, F.; Sattelmayer, T. ddtFoam. Available online: https://sourceforge.net/projects/ddtfoam/ (accessed on 1 March 2020).
19. Boeck, L.R.; Berger, F.M.; Hasslberger, J.; Ettner, F.; Sattelmayer, T. Macroscopic Structure of Fast Deflagrations and Detonations in Hydrogen-Air Mixtures with Concentration Gradients. In Proceedings of the 24th International Colloquium on the Dynamics of Explosions and Reactive Systems (ICDERS), Taipei, Taiwan, 28 July–2 August 2013; pp. 1–6.
20. Ogawa, T.; Oran, E.S.; Gamezo, V.N. Numerical study on flame acceleration and DDT in an inclined array of cylinders using an AMR technique. *Comput. Fluids* **2013**, *85*, 63–70. [CrossRef]
21. Kessler, D.A.; Gamezo, V.N.; Oran, E.S. Simulations of flame acceleration and deflagration-to-detonation transitions in methane-air systems. *Combust. Flame* **2010**, *157*, 2063–2077. [CrossRef]
22. Tieszen, S.R.; Sherman, M.P.; Benedick, W.B.; Lee, J.H. Detonation Cell Size measurements in H2-air-H_2O Mixtures. In Proceedings of the10th International Colloquium on Dynamics aof Explosions and Reactive Systems, Berkeley, CA, USA, 4–9 August 1985.
23. Dorofeev, S.B.; Sidorov, V.P.; Dvoinishnikov, A.E.; Breitung, W. Deflagration to detonation transition in large confined volume of lean hydrogen-air mixtures. *Combust. Flame* **1996**, *104*, 95–110. [CrossRef]
24. Ettner, F.A. Effiziente numerische Simulation des Deflagrations—Detonations—Übergangs. Ph.D. Thesis, Technische Universität München, Munich, Germany, 2013.

25. Weller, H.G.; Tabor, G.; Gosman, A.D.; Fureby, C. Application of a flame-wrinkling LES combustion model to a turbulent mixing layer. *Symp. Combust.* **1998**, *27*, 899–907. [CrossRef]
26. Conaire, M.O.; Curran, H.J.; Simmie, J.M.; Pitz, W.J.; Westbrook, C.K. A comprehensive modeling study of hydrogen oxidation. *Int. J. Chem. Kinet.* **2004**, *36*, 603–622. [CrossRef]
27. Malik, K.; Żbikowski, M.; Bąk, D.; Lesiak, P.; Teodorczyk, A. Numerical and experimental investigation of H_2-air and H_2-O_2 detonation parameters in a 9 m long tube, introduction of a new detonation model. *Int. J. Hydrog. Energy* **2019**, *4*, 8743–8750. [CrossRef]
28. Hasslberger, J.; Boeck, L.R.; Sattelmayer, T. Numerical simulation of deflagration-to-detonation transition in large confined volumes. *J. Loss Prev. Process. Ind.* **2015**, *36*, 371–379. [CrossRef]
29. Heidari, A.; Wen, J.X. Numerical simulation of flame acceleration and deflagration to detonation transition in hydrogen-air mixture. *Int. J. Hydrog. Energy.* **2014**, *39*, 21317–21327. [CrossRef]
30. Teodorczyk, A. Scale effects on hydrogen-air fast deflagrations and detonations in small obstructed channels. *J. Loss Prev. Process. Ind.* **2008**, *21*, 147–153. [CrossRef]
31. Rudy, W.; Teodorczyk, A. DDT limits in H_2-air mixture ina tube filled with obstacles. In Proceedings of the 27th ICDERS, Beijing, China, 28 July–2 August 2019; p. 277.
32. Toro, E.F.; Spruce, M.; Speares, W. Restoration of the contact surface in the HLL-Riemann solver. *Shock Waves* **1994**, *4*, 25–34. [CrossRef]
33. OpenFOAM, User Guide, Version 2.1.1. Available online: http://www.openfoam.org (accessed on 1 March 2019).
34. OpenFOAM Wiki, Limiters. 2010. Available online: https://openfoamwiki.net/index.php/OpenFOAM_guide/Limiters (accessed on 1 March 2019).
35. Goodwin, D.; Moffat, H.; Speth, R. Cantera: An Object-Oriented Software Toolkit for Chemical Kinetics, Thermodynamics, and Transport Processes. Available online: www.cantera.org (accessed on 1 June 2018).